Anchoring of intratumorally administered cytokines to collagen safely potentiates systemic cancer immunotherapy

Noor Momin[1,2], **Naveen K. Mehta**[1,2,†], **Nitasha R. Bennett**[1,†], **Leyuan Ma**[1,6,†], **Joseph R. Palmeri**[1,3], **Magnolia M. Chinn**[1,2], **Emi A. Lutz**[1,2], **Byong Kang**[1,2], **Darrell J. Irvine**[1,2,4,5,6], **Stefani Spranger**[1,7], **K. Dane Wittrup**[1,2,3,*]

[1.]Koch Institute for Integrative Cancer Research, Massachusetts Institute of Technology, Cambridge, MA 02142, USA.

[2.]Department of Biological Engineering, Massachusetts Institute of Technology, Cambridge, MA 02142, USA.

[3.]Department of Chemical Engineering, Massachusetts Institute of Technology, Cambridge, MA 02142, USA.

[4.]Ragon Institute of Massachusetts General Hospital, Massachusetts Institute of Technology and Harvard University, Cambridge, MA 02139, USA.

[5.]Department of Materials Science and Engineering, Massachusetts Institute of Technology, Cambridge, MA 02142, USA.

[6.]Howard Hughes Medical Institute, Chevy Chase, MD 20815, USA.

[7.]Department of Biology, Massachusetts Institute of Technology, Cambridge, MA 02142, USA.

Abstract

The clinical application of cytokine therapies for cancer treatment remains limited due to severe adverse reactions and insufficient therapeutic effects. Although cytokine localization by intratumoral administration could address both issues, the rapid escape of soluble cytokines from the tumor invariably subverts this effort. We find that intratumoral administration of a cytokine fused to the collagen-binding protein lumican prolongs local retention and dramatically reduces systemic exposure. Combining local administration of lumican-cytokine fusions with systemic immunotherapies (tumor-targeting antibody, checkpoint blockade, cancer vaccine, or T cell therapy) improves efficacy without exacerbating toxicity in syngeneic tumor models and the *Braf^V600E/Pten^fl/fl* genetically engineered melanoma model. Notably, curative abscopal effects on non-cytokine-injected tumors were also observed as a result of a protective and systemic CD8+ T cell response primed by local therapy. Cytokine collagen-anchoring constitutes a facile, tumor-agnostic strategy to safely potentiate otherwise marginally effective systemic immunotherapies.

*Corresponding Author. wittrup@mit.edu.

One-sentence summary:

Collagen-localized IL-2 and IL-12 cytokines potentiate disparate systemic cancer immunotherapies while minimizing toxicity in several tumor models.

Introduction

Cytokines that amplify and coordinate immune cell responses for tumor control can robustly synergize with other immunotherapies (1). Two such cytokines are interleukin-2 (IL-2) and interleukin-12 (IL-12), which expand and stimulate T cells and natural killer (NK) cells to mediate anti-tumor immunity. Despite their promising therapeutic effects, dose-limiting toxicity curbs the efficacy and the clinical translation of these cytokine therapies. The adoption of high-dose IL-2 therapy, despite its FDA approval, is limited by severe adverse effects. IL-12 therapies have not advanced to Phase 3 clinical trials due to toxicity. Efforts to engineer these cytokines to safely capitalize on their therapeutic potential are underway.

Ultimately, a cytokine's therapeutic index could be improved by localizing its effects to the tumor and away from healthy tissue. However, even when administered directly into a tumor, cytokines rapidly escape and enter systemic circulation in minutes, thus failing to fully address issues of toxicity and limited efficacy (2, 3). Recent efforts have shown that local injections of other immunomodulatory agents retained in or around a tumor lesion can improve efficacy and reduce systemic exposure (4-6).

To this end, we have developed a strategy to physically retain injected cytokine fusion proteins upon intratumoral injection, limiting their systemic dissemination while prolonging and localizing their therapeutic anti-tumor activity. We hypothesized that collagen, which is abundantly and ubiquitously expressed in tumors (7, 8), would be an effective and generalizable target for intratumoral localization. To devise collagen-anchoring cytokines, we fused IL-2 and IL-12 to lumican, a collagen-binding protein. Intratumorally administered collagen-anchoring IL-2 and IL-12 demonstrated prolonged intratumoral retention and effectively eliminated systemic exposure toxicity compared to locally-injected non-anchoring versions. Tumor-localized, lumican-cytokine fusions amplified systemic cellular anti-tumor immunity when combined with several marginally efficacious systemic immunotherapies: a tumor-targeting antibody, vaccine, chimeric antigen receptor (CAR)-T cell therapy, and neoadjuvant preoperative PD-1 checkpoint blockade in several syngeneic tumor models and the $Braf^{V600E}/Pten^{-/-}$ genetically engineered mouse model (GEMM) of melanoma. These results demonstrate that locally-administered collagen-anchoring cytokines safely potentiate systemic immunotherapies.

Results

Lumican fusions bind collagens I and IV and are intratumorally retained but systemically isolated

In search of an anchor for our localization strategy, we evaluated several collagen-binding proteins (9-13) (Fig. 1A). Issues with protein expression (fig. S1) and immunogenicity concerns narrowed the shortlist to lumican, an endogenous proteoglycan that assists in

collagen fibril assembly (12). Lumican is a stable protein (14) (fig. S2, A-B) that binds specifically to collagen types I and IV (Fig. 1B). Collagen I and IV are components of the thick fibrotic capsule surrounding tumors and the perivascular basement membrane, respectively (fig. S3). Intratumorally-injected fluorescently-labeled lumican colocalized with both collagen types in B16F10 tumors (Figs. 1, C to D). Although its expression and distribution vary, collagen is present in many syngeneic tumor models (7), and is thereby a tumor-agnostic target.

Having confirmed lumican's ability to bind collagen, we next assessed whether fusion to lumican improves the intratumoral retention of a payload. Ultimately, several factors dictate the intratumoral retention of a lumican-cytokine fusion protein: collagen binding affinity, collagen concentration, size-dependent escape by diffusion or convection, and cytokine receptor-mediated consumption. Although lumican's affinity for collagen (Kd > 100 nM) is relatively weak (Fig. 1B), high collagen abundance can drive complexation. To evaluate the retention imparted by collagen-anchoring, we fused lumican to mouse serum albumin (MSA). We monitored the persistence of fluorescently-labeled Lumican-MSA to MSA after intratumoral injection into apigmented B16F10 tumors using in vivo fluorescence imaging (Fig. 1, E and F). By 24 hours after injection, nearly all MSA had disappeared, whereas Lumican-MSA was still retained (Fig. 1, E and F). The fitted half-life in fluorescence of Lumican-MSA ($t_{1/2}$ = 24 hours) was slower than for MSA ($t_{1/2}$ = 5.2 hours). Lumican alone (37 kDa, $t_{1/2}$ = 16 hours) exits the tumor faster than Lumican-MSA (104 kDa), presumably due its smaller size, but still is retained better than MSA (67 kDa) (fig. S4). These results collectively demonstrate that collagen-binding affinity and molecular weight both contribute to prolonged intratumoral persistence of a fused payload.

To evaluate the extent to which the lumican-collagen interaction inhibits systemic dissemination of a fused payload, we compared the serum fluorescence of mice intratumorally injected with fluorescently-labeled Lumican-MSA to MSA (Fig. 1E). Twelve hours after intratumoral injection, 25% of the injected dose of MSA and 3% of the injected dose of Lumican-MSA was detected in the serum (Fig. 1G). Based on the area under the curve over five days after injection (Fig. 1G), fusion to lumican reduced MSA's systemic exposure by ten-fold.

Collagen-anchored IL-2 potentiates efficacy of a tumor-targeting antibody

IL-2 is a compelling candidate for tumor localization because its anti-tumor efficacy requires sustaining a high intratumoral concentration (15). Extended systemic IL-2 exposure potentiates the efficacy of anti-tumor antibodies (16, 17), adoptive T cell transfer(16), and combination immunotherapies with checkpoint blockade and anti-tumor vaccines (18). We explored the therapeutic effect of prolonging IL-2's intratumoral retention by collagen-anchoring.

IL-2 was expressed as a fusion to the C-terminus of Lumican-MSA, Lumican-MSA-IL2 (fig. S5A) and confirmed to bind intratumoral collagen in vivo (fig. S5B). MSA was incorporated to ensure steric access of receptors to IL-2 when bound to collagen fibrils, and also to increase the construct's molecular weight and thereby reduce diffusive flux away from the tumor. As an equivalently-bioactive comparator (fig. S6), IL-2 was also expressed as a

fusion to MSA (MSA-IL2) (fig. S5A), allowing the effects of collagen-binding to be largely separated from size-based improvements in tumor retention of small cytokines like wild-type IL-2 (16, 19, 20). We treated mice bearing established subcutaneous flank B16F10 melanoma tumors with an antibody against tyrosinase-related protein-1 (anti-TYRP-1, or TA99) intraperitoneally and/or with an intratumoral injection of an IL-2 fusion protein. Treatment with either Lumican-MSA-IL2 or MSA-IL2 provided modest tumor growth delay (fig. S7A); and Lumican and TA99 provided no benefit (fig. S7 A-B, Fig. 2A). In contrast, simultaneous administration of TA99 and IL-2 showed significant efficacy (p<0.0001), with the majority (15 of 17) of Lumican-MSA-IL2-injected mice cured, but very few (4 of 17) of those injected with MSA-IL-2 cured (Fig. 2A). After cessation of treatment, nearly all (16 of 17) mice injected with Lumican-MSA-IL2 developed vitiligo localized at the site of tumor inoculation, whereas only one of 17 MSA-IL2 treated mice displayed vitiligo (Fig. 2, B to C). Vitiligo coincides with the observation of an anti-melanocyte T cell response (21).

We evaluated the efficacy of TA99 treatment plus Lumican-MSA-IL2 injected into other anatomical sites: peritumorally (adjacent to the lesion) (Fig. 2D), intranodally (into the tumor-draining inguinal lymph node) (fig. S8), or subcutaneously at the tail base, 2 cm distal to the tumor site (Fig. 2D). Lumican-MSA-IL2 required intratumoral localization for maximal efficacy.

Lumican-MSA-IL2 and TA99 prime a curative tumor-specific T cell response

Given IL-2's broad effects, we sought to determine the contributions of distinct immune cells and soluble factors to Lumican-MSA-IL2's therapeutic efficacy by antibody-mediated depletions or in *Batf3*$^{-/-}$ mice that are deficient in cross-presenting dendritic cells (DCs). Depletion of NK cells, neutrophils, eosinophils, or macrophages did not alter efficacy (Fig. 2E, fig. S9), indicating that no single tested innate cell population was independently responsible for tumor control. However, CD8+ T cells, cross-presenting DCs, and interferon-gamma (IFN-γ) were critical for tumor rejection (Fig. 2E).

Because earlier studies indicated that systemic adaptive immune activation is required for effective therapy (22), the localized patch of vitiligo raised the question of whether a tumor-specific T cell response could be detected outside the treated lesion. An IFN-γ ELISPOT on splenocytes harvested four days after treatment with TA99 and IL-2 revealed tumor-specific T cells in the spleen. Notably, treatment with Lumican-MSA-IL2 yielded nearly four-fold more tumor-specific T cells in the spleen than diffusible MSA-IL2 (Fig. 2F). We used intracellular cytokine staining for IFN-γ on splenocytes to confirm that this response was generated by tumor-specific CD8+ T cells (fig. S10, A-B). These results show that Lumican-MSA-IL2, although tumor-localized, mobilizes a greater systemic tumor-specific response than its unanchored equivalent, MSA-IL2. In fact, the majority (9 of 15) of long-term survivors of TA99 and Lumican-MSA-IL2 treatment rejected a rechallenge with B16F10 inoculated on the contralateral flank, indicative of the formation of effective systemic immunological memory with this therapy (fig. S10C).

Next, we probed for the capacity of the peripheral effectors induced by the combination of TA99 and localized IL-2 treatment to control a concurrent distant lesion (23). We inoculated B16F10 tumors subcutaneously on both flanks and administered TA99 systemically but IL-2

intratumorally only into the right, or ipsilateral, tumor. The combination with MSA-IL2, which can leak out of the ipsilateral tumor and to the contralateral lesion after injection, imparted some contralateral tumor control but most mice succumbed to tumor burden (Fig. 2G). Conversely, the combination with Lumican-MSA-IL2, which is isolated to the ipsilateral tumor, halted ipsilateral and contralateral tumor growth, resulting in durable cures in most (4 of 7) mice (Fig. 2G). The antitumor response elicited by anchoring IL-2 in a single tumor is superior in controlling and eradicating disseminated disease than systemic exposure of the same IL-2 dose.

IL12-MSA-Lumican eliminates treatment-related weight loss

Next, we applied this localization platform to another toxicity-limited cytokine, IL-12. IL-12 acts as a key regulator in Th1 cell mediated immunity, which is critical for effective anti-tumor responses. Unfortunately, severe toxicities and fatalities halted an early clinical trial administering systemic IL-12 (24). IFN-γ, induced by IL-12 stimulation of NK and T cells, was implicated in the toxicity but is also inextricably coupled to IL-12's efficacy (25). We hypothesized that localizing IL-12 to the tumor would ameliorate this toxicity.

We constructed wild-type murine IL-12 p40 and p35 subunits in a single-chain format (scIL12). To create a collagen-anchoring version of IL-12, we expressed scIL12 at the N terminus of MSA-Lumican fusion, henceforth IL12-MSA-Lumican (fig. S11, A-B). For comparison, we used IL12-MSA, a non-anchoring version of scIL12 (fig. S11, A-B).

Intratumoral administration of IL12-MSA in B16F10 tumor-bearing mice led to significant (p < 0.002) weight loss, a proxy for toxicity (Fig. 3A). Systemic administration of IL12-MSA via intraperitoneal injection resulted in identical weight loss (Fig. 3A). In contrast, an equimolar intratumoral injection of IL12-MSA-Lumican did not cause weight loss (Fig. 3A). These results demonstrate that local administration without an effort towards retention is insufficient to alleviate toxicity, and collagen-anchoring provides sufficient intratumoral confinement to curb systemic toxicities of IL-12.

IL12-MSA-Lumican safely potentiates a cancer vaccine, CAR-T cell therapy, and neoadjuvant checkpoint blockade

Monotherapy with IL-12 delayed tumor outgrowth but was not curative (Fig. 3B). Several synergistic combinations to potentiate the anti-tumor effects of IL-12 have been proposed but suffer from prohibitive supra-additive toxicities (26). To enable its safe use in combination strategies, groups have devised DNA- (27), cell- (28), or materials-based (29) methods intended to locally confine IL-12 activity. In these forms, IL-12 has enhanced the efficacy of cancer vaccines, CAR-T cell therapy, and neoadjuvant checkpoint blockade. We sought to evaluate our recombinant protein-based approach to IL-12 localization in combination with these same immunotherapies. Anticipating toxicities arising in combination treatments, we reduced the IL-12 dose to a tenth of that administered in Fig. 3A-B (fig. S12).

Intratumoral electroporation of IL-12-encoding DNA is being investigated clinically as a vaccine adjuvant in melanoma (27). We speculated that tumor-collagen-localized IL-12 could analogously potentiate T cells primed by an effective anti-tumor vaccine.

Subcutaneous administration of cyclic-di-nucleotide adjuvant and a lymph-node-targeting moiety (30) fused to B16F10-associated peptide antigens TYRP-1 and EGP primed an antigen-specific CD8+ T cell response (fig. S13). The vaccination alone modestly delayed B16F10 tumor growth; however, coadministration with IL-12, using either IL12-MSA or IL12-MSA-Lumican, prolonged tumor control, with IL12-MSA-Lumican extending survival longer than IL12-MSA (Fig. 3C). Additionally, vaccination with IL12-MSA caused weight loss that was not observed with IL12-MSA-Lumican.

IL-12 also amplifies CAR-T efficacy, as observed with autocrine IL-12-expressing "armored" CAR-T (28). However, the lack of stringent spatiotemporal expression of IL-12 in such cell therapies can lead to marked toxicity as seen in two terminated clinical trials (NCT01236573, NCT01457131) using IL-12-engineered T cells, a concern potentially averted by intratumoral administration of collagen-anchoring cytokines. B16F10-specific CAR-T cells were generated by transducing CD3+ splenocytes to express a CAR composed of single-chain variable fragment (scFv) of TA99 fused to costimulatory CD28 and CD3ζ signaling domains. To ensure CAR-T cell engraftment, all mice were preconditioned with total body irradiation the day before a single bolus injection of 10 million CAR-T cells. Treatment with CAR-T cells or IL-12 alone only delayed tumor growth. However, the combination of CAR-T cells and IL-12, as either IL12-MSA or IL12-MSA-Lumican, demonstrated increased survival. However, only CAR-T cell therapy combined with IL12-MSA-Lumican produced durable tumor regression (Fig. 3D) and prominent vitiligo in every mouse treated. Additionally, IL12-MSA caused weight loss that was not observed with IL12-MSA-Lumican (Fig. 3D).

Intratumoral neoadjuvant immunotherapy using anti-PD-1 checkpoint blockade (31) and biomaterial-embedded IL-12 has demonstrated efficacy in controlling recurrence and metastases (29). We hypothesized that collagen-anchored IL-12 could recapitulate these effects in the spontaneously metastasizing tumor model 4T1. Luciferase-expressing 4T1 breast tumor cells (4T1-Luc) were implanted into the mammary fat pad. Before surgical resection of this lesion, mice were treated with IL-12 intratumorally and anti-PD-1 systemically. The neoadjuvant therapy with IL12-MSA-Lumican resulted in more primary tumor debulking than the non-anchoring version scIL12. After primary tumor resection surgery, mice were monitored for metastases by in vivo bioluminescence imaging. IL12-MSA-Lumican completely protected mice from metastatic growth, whereas several mice treated with scIL12 relapsed (Fig. 3E). These results demonstrate that collagen-anchoring IL-12 in a neoadjuvant setting can improve postoperative metastasis outcomes.

IL12-MSA-Lumican plus Lumican-MSA-IL2 cures B16F10 tumors without systemic toxicity

Collagen anchoring IL-2 or IL-12 safely potentiated the effects of a tumor-targeting antibody (Fig. 2A), cancer vaccine (Fig. 3C), CAR-T cell therapy (Fig. 3D), and neoadjuvant checkpoint blockade (Fig. 3E). The first three of these therapies require *a priori* knowledge of expressed tumor antigens to inform their development. Having devised a generalizable approach for cytokine localization, we next explored combinations using exclusively tumor-agnostic agents.

IL-2 and IL-12 engage complementary signaling pathways in NK and T cells (32, 33). Furthermore, IL-2 upregulates the expression of IL-12 receptor subunit β (34), and IL-12 sustains surface expression of IL-2 receptor CD25 (35). This reciprocity augments the effects of IL-2 and IL-12. Despite promising efficacy, several clinical trials of this combination have been terminated (32, 36). Notably, this combination also greatly enhances lymphocyte production of IFN-γ (32). Therefore, in addition to mutual potentiation, we anticipated that, unless collagen-anchored, these cytokines would cause substantial systemic toxicity (37).

As single agents dosed intratumorally, the reduced doses of IL12-MSA and MSA-IL2 neither cause weight loss (fig. S14) nor overall survival enhancement (Fig. 3 C to E, fig. S7) in B16F10 tumor-bearing mice. However, as anticipated, the combination of unanchored IL12-MSA and MSA-IL2 resulted in significant (p < 0.0001) weight drop and modest overall survival (Fig. 4A). In comparison, the collagen-anchoring versions, IL12-MSA-Lumican and Lumican-MSA-IL2, did not cause weight loss and resulted in the survival of 3 of 5 mice (Fig. 4A). Collagen-anchoring IL-2 and IL-12 curbed the treatment-related toxicity and, moreover, tapped into the curative potential of this cytokine combination (Fig. 4A) at doses where the monotherapies were ineffective (Fig. 3 C to E, fig. S7).

We examined which immune cells were responsible for the efficacy of intratumoral IL12-MSA-Lumican and Lumican-MSA-IL2 combination. Based on antibody-mediated depletions during the course of treatment in B16F10 tumor-bearing wild type and *Batf3*^{−/−} mice, we found CD8+ T cells and cross-presenting dendritic cells to be indispensable for efficacy (fig. S15A). Individual depletion of NK cells, neutrophils, eosinophils, or macrophages did not significantly affect the survival outcome (fig. S15B). Surprisingly, blocking IFN-γ, known to be amplified by concurrent IL-2 and IL-12 stimulation, also did not significantly alter survival (fig. S15A). This lack of effect might be attributed to insufficient depletion of excessive IFN-γ produced. Completely neutralizing IFN-γ is challenging due to the short distance between a nascently secreted IFN-γ and its receptor, which is expressed on all nucleated cells. Notably, within the cohort given the IFN-γ depletion antibody, we observed a bimodal effect on early tumor growth, suggesting some therapeutic role of this cytokine (fig. S15C). In comparing immune cell infiltrates between IL12-MSA and MSA-IL2 treated versus IL12-MSA-Lumican and Lumican-MSA-IL2 treated tumors, the difference in CD8+ T cells was most striking (fig. S16, A-D). Tumors treated with the lumican-cytokine fusions had more infiltrating CD8+ T cells compared to tumors treated with the unanchored cytokines six days after initial treatment (Fig. 4B). However, these effectors had higher surface expression of PD-1, a T cell exhaustion marker (Fig. 4B).

Tumor-agnostic IL-12 and IL-2 combination enhances PD-1 checkpoint blockade

Given the upregulation of surface PD-1 on tumor-infiltrating CD8+ T cells in response to lumican-cytokine treatment, we tested whether this local cytokine therapy could synergize with systemic PD-1 checkpoint blockade. Because we also observed tumor-specific T cells in the periphery six days after the first treatment with IL-2 and IL-12 (fig. S16E), we chose to administer anti-PD-1 systemically to alleviate intratumoral and peripheral

immunosuppression. The inclusion of anti-PD-1 did not alter the weight loss patterns observed previously for this treatment (Fig. 4, A and C), but the addition of anti-PD-1 improved survival outcomes for mice treated with IL12-MSA and MSA-IL2. Although anti-PD-1 administration did not further improve survival for IL12-MSA-Lumican and Lumican-MSA-IL2 treated mice, localized vitiligo occurred more frequently when anti-PD-1 was given alongside lumican-cytokines (Fig 4D). Additionally, more survivors from cytokine and anti-PD-1 treatment (6 of 6 mice) compared to survivors from cytokine treatment alone (1 of 3 mice) were protected against a subsequent tumor rechallenge with B16F10 (Fig. 4E). Inclusion of anti-PD-1 in this therapy increased the occurrence of treatment-induced vitiligo (Fig. 4D) and effective memory (Fig. 4E), thus demonstrating its role in enhancing T cell responses generated from localized IL-2 and IL-12 treatment. Despite the potency, treatment did not generate endogenous antibodies against the administered fusion proteins, indicating that these agents are immune-activating but not themselves antigenic (fig. S17).

Prior findings regarding the specific mechanism of action for IL-12 mediated tumor control varied depending on the tumor type and/or location (38, 39). We speculated whether this cytokine combination would be effective in other syngeneic tumor models. Because collagen is expressed ubiquitously across all solid tumors, IL12-MSA-Lumican and Lumican-MSA-IL2 could be tumor-antigen-agnostic immunotherapies. Generally, tumors can be prognostically classified into phenotypes including "immune desert", "immune excluded," or "inflamed" based on their T cell infiltration (1). B16F10 melanoma (Fig. 4, A-E), is poorly immunogenic and therefore demonstrates an "immune desert" phenotype (40). The metastatic 4T1 breast model treated with IL-12, anti-PD-1, and surgery in Fig. 3E is strongly immunogenic and immune cell-infiltrated, and thereby recapitulates an "inflamed" phenotype (40). To evaluate the generalizability of lumican-cytokines and PD-1 checkpoint blockade to "immune excluded" tumors, we used the EMT6 mammary carcinoma and the MC38 colon carcinoma models (41). Treatment of either EMT6 (Fig. 4F) or MC38 (Fig. 4G) lesions with IL12-MSA-Lumican and Lumican-MSA-IL2 and systemic anti-PD-1 achieved survival improvements.

IL12-MSA-Lumican, Lumican-MSA-IL2, anti-PD-1, and TA99 demonstrate efficacy in Braf^{V600E}/Pten$^{fl/fl}$ GEMM

Since syngeneic tumors poorly recapitulate the progression and pathophysiology of human cancers, we tested the effectiveness of lumican-cytokines in the *Braf^{V600E}/Pten$^{fl/fl}$* GEMM. Melanomas in this GEMM are induced by tamoxifen-regulated Cre expression in melanocytes, which drives the activation of oncogenic *Braf^{V600E}* and biallelic deletion of tumor suppressor *Pten*. This model has modest T cell infiltration, but growth is only slightly slowed by dual checkpoint blockade using anti-PD-1 and anti-CTLA-4 (42). We thought treatment with IL-2 and IL-12 alongside anti-PD-1 checkpoint blockade could reinvigorate the ongoing response and prime new T-cell responses, as we observed in B16F10 tumors (Fig. 4). However, considering that *Braf^{V600E}/Pten$^{fl/fl}$* melanomas possess fewer neoantigens and more heterogeneity than B16F10 tumors, we hypothesized that *de-novo* T-cell priming and any abscopal effects could be augmented by the inclusion of an immunogenic-cell-death-directing agent like the tumor-targeting antibody TA99 (1, 43)(42)(44).

We induced tumors on the right flank of *Braf^V600E^/Pten^fl/fl^* mice and waited to treat until large black lesions had formed. In the absence of therapy, the initially flat pigmented lesions progressed to large masses. However, treatment with intratumoral IL12-MSA-Lumican and Lumican-MSA-IL2 alongside systemic anti-PD-1 and TA99 halted tumor growth (Fig. 5, A-B).

Despite its efficacy in this difficult-to-treat GEMM, the translatability of this combination treatment is limited by the dearth of clinically available tumor-targeting antibodies. Comparing the overall survival of *Braf^V600E^/Pten^fl/fl^* tumor-bearing mice treated with anti-PD-1 and collagen-anchoring IL-2 and IL-12 with or without TA99, we found that TA99 was not a necessary component for efficacy (Fig. 5C). These results affirm our earlier findings (Fig. 4) that IL-2, IL-12, and checkpoint blockade can be an effective tumor-agnostic combination treatment.

Additionally, we found that tumor control in this model could also be achieved using unanchored cytokines in lieu of collagen-anchoring cytokines, but at the cost of major and potentially lethal toxicity. One-third of the mice treated with IL12-MSA and MSA-IL2 were euthanized due to >20% loss of body weight, whereas no mice treated with IL12-MSA-Lumican and Lumican-MSA-IL2 succumbed to treatment-related toxicity (Fig. 5C). With collagen-anchoring, this potent tumor-agnostic combination treatment can safely improve overall survival (Fig. 5C).

Discussion

It has been an outstanding challenge to unleash cytokines' anti-tumor therapeutic efficacy without exacerbating toxicity. Here we demonstrate that collagen-anchoring of IL-2 and IL-12 by fusion to lumican is a tumor-agnostic protein-based strategy to potentiate immunotherapy while also ameliorating systemic toxicity.

The inherent challenge of limiting exposure of patients to systemic cytokines has prompted investigation into local administration of wild-type cytokines. Studies, however, show that a local injection does not prevent cytokine leakage. In humans, high concentrations of IL-12 (2) and IL-2 (3) were measured in circulation 3 hours after subcutaneous/intratumoral administration, thereby undermining the posited advantages (high concentration and low toxicity) of local delivery. The rapid escape of locally injected wild-type cytokines out of the tumor is largely a consequence of their small size (IL-2 is 16 kDa and IL-12 is 57 kDa). Among the improvements made to cytokines, fusion to large biomolecules such as albumin or polyethylene glycol has been successfully used to extend cytokine persistence in circulation (19). Although cytokine fusion to MSA (MSA-IL2 and IL12-MSA) analogously increases passive tumor retention upon local injection, we found the efficacy and safety profile of combinations with MSA-cytokine fusions consistently inferior to those achieved using lumican-MSA-cytokine fusions. Local delivery and prolonged passive size-based retention do not endow cytokines with the prolonged intratumoral persistence or systemic isolation necessary to maximize therapeutic index.

There have been numerous efforts to improve the therapeutic index of cytokines by targeting. Most commonly, cytokines have been fused to tumor-targeting antibodies, a format called immunocytokines. However, such immunocytokines generally first extend a cytokine's systemic exposure before diffusion into the tumor (20) and as a result, often still suffer from dose-limiting systemic toxicities (45, 46). Smaller immunocytokines may demonstrate better tumor-targeting efficiency due to rapid renal clearance (20, 47), but may also therefore require frequent dosing to maintain therapeutic intratumoral concentrations. At first glance, administering immunocytokines intratumorally may seem like a solution. However, nearly all clinical tumor-targeting monoclonal antibodies engage cell surface receptors that undergo internalization (48). The steady-state internalization of these cellular targets undercuts a cytokine's receptor-accessible tumor residence time and efficacy. Targeting an acellular antigen, such as a component of the extracellular matrix, minimizes constitutive target-mediated depletion of a cytokine fusion (49). Currently, tumor-targeting scFv against splice variants of the matrix proteins fibronectin and tenascin C are under development as fusions to IL-2 and tumor necrosis factor alpha (50). Preclinical investigation of these agents had primarily relied on systemic routes of administration. However, in a phase II clinical trial, these immunocytokines were administered intralesionally and were well tolerated with moderate efficacy (50, 51). Although their local administration is promising, immunocytokines are also generally restricted and dose-limited by variable target expression (46, 52) unlike collagen, a ubiquitous and highly abundant protein.

Although both tumors and healthy tissues contain collagen, intratumoral administration eliminates the need to target a tumor-specific antigen. Instead, to maximize retention and confinement of our cytokine payload, we prioritized high abundance (8) and slow turnover (49) when selecting our target. Collagen types I and IV are among the most prevalent components of the matrix in most tissues and tumors (8). Although collagen density varies across tumor types, lumican-cytokines proved efficacious in tumor models with <3% collagen (B16F10 and $Braf^{V600E}/Pten^{fl/fl}$), 5% collagen (MC38), 10% collagen (EMT-6), and 20% collagen (4T1) (7, 53). These tumor models include all three immune phenotypes: desert (B16F10 and $Braf^{V600E}/Pten^{fl/fl}$), excluded (MC38 and EMT-6), and inflamed (4T1) (40). Collagen-anchoring is therefore a tumor-agnostic strategy permissive to a range of collagen density and to differential immune infiltration status.

Collagen types I and IV demonstrate distinct intratumoral spatial distributions that may have also contributed to the improved therapeutic efficacy of lumican-cytokine fusions. Collagen type I deposition at the tumor's invasive margin has been clinically observed in several cancers including breast (54), colorectal (55), and skin (56). Typically the invasive margin has more immune cells, particularly T cells, compared to the center of the tumor (57). Matrix-embedded lymphocytes also preferentially "crawl" along collagen fibers (58). Therefore, by anchoring to collagen type I, lumican-cytokines are effectively concentrated in areas dense with effector lymphocytes and potentially along their migration tracks. Additionally, lumican colocalization with collagen IV at the basement membrane of blood vessels may poise lumican-cytokines to stimulate extravasating immune cells (50, 59, 60). The exact impact of alternative spatial distribution (localization to collagen type I vs. type IV) on the therapy-potentiating effects remains to be determined.

Clinical translation of intratumorally administered therapies is growing rapidly: small-molecule agonists (61), plasmids, and viruses (62) have all been intratumorally administered into stage III/IV melanoma tumors. For translation to other indications, the issue is whether the return on investment (in terms of improved efficacy and reduced toxicity) is worth the increased logistical effort of intratumoral administration. Another concern for locoregional immunotherapy is the effective control of disseminated metastases. In this regard, our demonstration of durable and systemic anti-tumor responses in a contralateral non-injected tumor and neoadjuvant reduction of post-resection metastases is encouraging. These results suggest that robust local immune stimulation may be essential for curative abscopal effects. It is likely that the greatest benefits will be obtained by combining both systemic and localized therapies, such that a vigorous local immune activation can engender a systemic adaptive response that cooperates with systemic therapy.

To demonstrate the concept of collagen-anchoring localization, we limited our investigation to two cytokines: IL-2 and IL-12. Furthermore, the dosing of IL-2 and IL-12 or their molar ratio had not been empirically optimized. These cytokines may benefit from further investigation, and other immunotherapies altogether may benefit from tumor-localization. Fortunately, as a tumor- and payload- agnostic platform, lumican is amenable to fusion to other immunomodulatory payloads and translation to several solid tumor models.

Materials and Methods

Study design

The objectives of this work were to 1) develop a generalizable recombinant-protein strategy that relies on collagen-anchoring to improve the therapeutic index of locally-injected cytokines and 2) compare the efficacy and toxicity of intratumorally-injected collagen-anchoring cytokines to unanchored cytokines in combination treatments.

Multiple individuals on separate occasions recombinantly expressed and purified the cytokine-fusions proteins for therapeutic studies in mice. The studies conducted in subcutaneous syngeneic B16F10 tumors tested for potentiation of a systemic immunotherapy by local cytokine therapy as well as compared the effectiveness and safety of collagen-anchoring cytokines to non-anchoring cytokines. The therapeutic studies conducted in subcutaneous MC38, EMT6, and 4T1 tumors assess the tumor-agnostic efficacy of collagen-anchoring cytokines. The $Braf^{V600E}/Pten^{fl/fl}$ melanoma GEMM demonstrated the translatability of collagen-anchoring cytokines in a clinically relevant model.

In all studies, tumor-bearing mice were randomized before the first treatment to ensure similar tumor sizes across treatment groups and were monitored for tumor size and weight loss until euthanasia. We did not use a power analysis to preemptively calculate sample size. Experimental cohorts were composed of at least 5 but typically 7 mice per group; experiments were typically repeated at least twice, and results were pooled for analysis. For each experiment, numbers of mice and experimental replicates are stated in the figure legend. Samples were not excluded from analysis, and investigators were not blinded during the experiments.

Mice

B6 mice (C57BL/6NTac) and Balb/C (BALB/cAnNTac) were purchased from Taconic, and *Batf3*$^{-/-}$ (B6.129S(C)-*Batf3*^{tm1Kmm}/J) were purchased from the Jackson Laboratory. Balb/C mice used in 4T1 orthotopic tumor model were purchased from Jackson Laboratory. Tyr:Cre-ER^{+}/LSL-*Braf*^{V600E}/*Pten*$^{fl/fl}$ mice (designated *Braf*^{V600E}/*Pten*$^{fl/fl}$) were generated by T. F. Gajewski (University of Chicago) from mouse strains obtained from L Chin, M. MacMahon, and T. Mak. *Batf3*$^{-/-}$ and *Braf*^{V600E}/*Pten*$^{fl/fl}$ mice were bred in-house and genotyped (Transnetyx). All animal work was conducted under the approval of the Massachusetts Institute of Technology Division of Comparative Medicine in accordance with federal, state, and local guidelines.

Cells

B16F10, EMT6, and 4T1 were purchased from ATCC. 4T1-GFP-Luc (4T1-Luc) cells were generated by transfection of the 4T1 cell line with pGreenFire lentiviral vector (System Biosciences). Apigmented B16F10 cells were generated by deleting tyrosinase-related protein-2 (TRP2), henceforth B16F10-TRP2 knockout (KO) (18). MC38 cells were a gift from J. Schlom (National Cancer Institute). Tumor cells were cultured in Dulbecco's modified Eagle's medium (ATCC) supplemented with 10% FBS (Thermo Fisher Scientific). HEK293 cells purchased from Life Technologies were cultured in Freestyle medium (Life Technologies). Cells isolated from the spleen or blood of B6 mice were cultured in RPMI-1640 (ATCC) with 10% FBS, 20 mM HEPES, 1 mM sodium pyruvate, 0.05 mM β-mercaptoethanol (Life Technologies), 100 units/ml penicillin (Life Technologies), 100 μg/ml streptomycin (Life Technologies), 2 mM L-alanyl,-L-glutamine (Life Technologies), and 1x minimal essential medium (Corning) non-essential amino acids. CTLL-2 cells purchased from ATCC were cultured in the same medium with 10% T cell culture supplement with concanavalin A (T-STIM with ConA, Corning). All cells and cell assays were maintained at 37°C and 5% CO_2. All cell lines were tested for mycoplasma contamination, and none tested positive.

Subcutaneous and orthotopic tumor inoculation and treatments

Mice were aged for 6-8 weeks before subcutaneous or orthotopic tumor inoculation. For inoculation of single B16F10, B16F10-TRP2KO, MC38, and EMT6 tumors, 10^6 cells in 50 μl of sterile PBS (Corning) were injected subcutaneously into the right flanks of C57BL/6 or Balb/C female mice with the exception of the CAR-T cell therapy study, where 0.5×10^6 B16F10 cells was used. For the orthotopic model, 0.5×10^6 4T1-Luc cells in sterile PBS were injected into the mammary gland of Balb/C female. For Fig. 2G, 10^6 B16F10 cells were injected subcutaneously into the right flank, denoted ipsilateral, and 0.3×10^6 B16F10 cells were injected subcutaneously into the left flank, denoted contralateral.

TA99 was administered at 100 μg per dose intraperitoneally (i.p.) in 100 μl of sterile PBS, and anti-PD-1 (clone 29F.1A12, BioXCell) was administered at 200 μg per dose i.p. in 50 μl of sterile PBS. Intratumoral treatments into the subcutaneous flank tumors were administered in 20 μl of sterile PBS. For all IL-2 treatments (equivalent of 0.11 nmol used), MSA-IL2 (84 kDa) was administered at 9 μg per dose (i.tu.) and Lumican-MSA-IL2 (121 kDa) was administered at 13 μg per dose (i.tu.). This IL-2 dose was informed by 1) the

previously optimized systemic MSA-IL2 (16) and 2) prediction that ~30% of a systemically injected dose of a cytokine-fusion protein achieves tumor localization (20). For most IL-12 treatments (equivalent of 14 pmol used), IL12-MSA (126 kDa) was administered at 1.78 μg per dose (i.tu.), and IL12-MSA-Lumican (163 kDa) was administered at 2.3 μg per dose (i.tu.). However, for Fig. 3A-B, the IL-12 dose used was 140 pmol. For the 4T1-Luc orthotopic surgery model in Fig. 3E, the IL-12 dose used was 30 pmol, such that 1.9 μg per dose of scIL12 (60 kDa) and 4.9 μg per dose of IL12-MSA-Lumican (163 kDa) was administered in 30 μl of sterile PBS alongside 200 μg of anti-PD-1 (clone RMP1-14, BioXCell) in 50 μl of sterile PBS.

The vaccine, composed of 90 μg of TTR-Trp1-EGP (30) and 50 μg of cyclic dinucleotides (Invivogen), was administered subcutaneously at the base of the tail, with half of the dose given on each side. CAR-T cell therapy entailed a tail-vein intravenous injection of 10 million mixed CD3+ cells into mice preconditioned with 500 cGy sublethal total body irradiation.

During therapeutic studies, mice were monitored continuously for weight changes and tumor growth by direct measurement or in vivo imaging until the euthanasia endpoint was reached: either 20% total body weight loss or 100 mm^2 tumor area (length x width) for B16F10, MC38, and EMT6 models; or metastasis-related morbidity in orthotopic 4T1 model. Mice that rejected tumors were re-challenged with 10^5 matched tumor cells on the left flank.

Surgical resection of 4T1-Luc primary tumor and subsequent metastasis monitoring

Surgical resection of primary 4T1-Luc tumor was performed 16 days after tumor inoculation. Mice were completely anesthetized with isoflurane, s.c. sustained-release buprenorphine (ZooPharm, 1 mg/kg body weight), and meloxicam (2 mg/kg body weight). The shaved surgical area was sterilized with alternating swabbing of betadine surgical scrub and 70% ethanol. The tumor and surrounding mammary fat pad was removed by blunt dissection using autoclaved surgical instruments (Braintree Scientific). Wounds were closed using 4-0 nylon monofilament sutures with a 3/8 reverse cutting needle (Ethilon). Mice were dosed with meloxicam (2 mg/kg body weight) at 24 hour intervals for 3 days after surgery. Sutures were removed at 7-10 days after the operation.

Mice were monitored for development of metastasis using bioluminescence imaging starting at 10-14 days after surgical resection of the primary tumor. Animals were injected i.p. with sterile-filtered D-luciferin (Xenogen) in PBS (150 mg/kg body weight in 200 μl) and imaged 10 minutes after D-luciferin injection with a IVIS Spectrum Imaging System 100 (IVIS, Xenogen). Animals were monitored daily for morbidity and euthanized if signs of distress, >20% body weight loss, or poor body condition (at veterinary staff discretion) were observed.

In vivo protein retention and pharmacokinetics

Proteins were labeled with Alexa Fluor 647 NHS Ester (Life Technologies). Excess dye was removed using a PD10 Desalting Column (GE Healthcare) and degree of labeling for each protein was calculated. Proteins compared in pharmacokinetic (PK) and retention studies contained equimolar dye. Lumican-MSA and MSA, 1.1 nmol of each (110 μg of Lumican-

MSA and 71.7 μg of MSA) was injected intratumorally into mice bearing B16F10-TRP2KO tumors five days after tumor inoculation. For Lumican-MSA-IL2 and MSA-IL2, 0.11 nmol, and for IL12-MSA-Lumican and IL12-MSA, 140 pmol of construct was injected.

To assess protein retention, mice were imaged with IVIS under auto-exposure epi-illumination fluorescence settings. During this time, mice were maintained on an alfalfa-free casein chow (Test Diet) to minimize gastrointestinal background fluorescence. Image analysis to determine total radiant efficiency was performed using Living Image (Caliper Life Sciences).

To assess pharmacokinetics after injection, <10 μl of blood was drawn into glass micro-hematocrit heparin-coated tubes (VWR) from the tip of the tail at indicated time points. Tubes were parafilm-sealed at one end and stored upright protected from the light at 4°C to allow serum separation from clotted blood by gravity. Tubes were scanned using a flatbed Typhoon Trio Variable Mode Imager (GE Healthcare), and serum fluorescence was quantified using Fiji image analysis software.

Antibody-mediated depletions

Cellular subsets were depleted by intraperitoneal (i.p.) administration of depleting antibody beginning one day before the first treatment until one week after the last treatment. CD8 T cells, NK cells, or neutrophils were depleted with 400 μg of anti-CD8-α (2.43, BioXCell), anti-NK1.1 (PK136, BioXCell), or anti-Ly-6G (1A8, BioXCell) every four days. Macrophages or IFN-y were depleted using 300 μg of anti-CSF1R (AFS98, BioXCell) or 200 μg of anti-IFN-y (XMG1.2, BioXCell) every other day. Eosinophils were depleted using 1 mg of anti-IL-5 (TRFK5, BioXCell) weekly.

Induction and treatment of *Braf^V600E^/Pten^fl/fl^* autochthonous melanoma

6-15-week-old Tyr:Cre-ER[+]/LSL-*Braf^V600E^/Pten^fl/fl^* mice were painted with 5 μl of 4-hydroxytamoxifen (Sigma) at 5 mg/ml dissolved in acetone on the right flank on day 0. On day 25, mice were treated with TA99 at 100 μg per dose intraperitoneally (i.p.) in 100 μl of sterile PBS, and anti-PD-1 (clone 29F.1A12, BioXCell) at 200 μg per dose i.p. in 50 μl of sterile PBS. For IL-2 treatment (equivalent of 0.33 nmol), 39 μg per dose of Lumican-MSA-IL2 or 27 μg per dose of MSA-IL2 was administered intratumorally. For IL-12 treatment (equivalent of 42 pmol), 6.9 μg per dose of IL12-MSA-Lumican or 5.4 μg per dose of IL12-MSA was administered intratumorally. Intratumoral injections were administered in 80 μl of sterile PBS along four distinct needle tracks. Tumor size was measured as volume (length x width x height), and mice were euthanized when tumors exceeded 1200 mm^3 or if body weight loss from treatment onset exceeded 20%.

Statistical analysis

Statistical analysis was performed with GraphPad Prism 8 software. Weight changes and other comparisons between groups were assessed by one-way ANOVA with Tukey's multiple comparison test. Kaplan-Meier survival curves were compared by log-rank Mantel-Cox test. Significance was represented as follows: *, $P < 0.03$; **, $P < 0.002$; ***, $P <$

0.0002; ****, P < 0.0001; n.s., not significant. The *n* values and specific statistical methods are indicated in figure legends. Original data are presented in data file S1.

Data and materials availability:

All data associated with this study are present in the paper or Supplementary Materials.

Supplementary Material

Refer to Web version on PubMed Central for supplementary material.

Acknowledgements:

References and Notes:

1. Chen DS, Mellman I, Elements of cancer immunity and the cancer-immune set point, Nature 541, 321–330 (2017). [PubMed: 28102259]

2. Eton O, Rosenblum MG, Legha SS, Zhang W, Jo East M, Bedikian A, Papadopoulos N, Buzaid A, Benjamin RS, Phase I trial of subcutaneous recombinant human interleukin-2 in patients with metastatic melanoma, Cancer 95, 127–134 (2002). [PubMed: 12115326]

3. Van Herpen CM, Huijbens R, Looman M, De Vries J, Marres H, Van De Ven J, Hermsen R, Adema GJ, De Mulder PH, Pharmacokinetics and immunological aspects of a phase Ib study with intratumoral administration of recombinant human interleukin-12 in patients with head and neck squamous cell carcinoma: a decrease of T-bet in peripheral blood mononuclear cells, Clin. Cancer Res 9, 2950–2956 (2003). [PubMed: 12912941]

4. Ishihara J, Fukunaga K, Ishihara A, Larsson HM, Potin L, Hosseinchi P, Galliverti G, Swartz MA, Hubbell JA, Matrix-binding checkpoint immunotherapies enhance antitumor efficacy and reduce adverse events, Sci. Transl. Med 9 (2017), doi:10.1126/scitranslmed.aan0401.

5. Sagiv-Barfi I, Czerwinski DK, Levy S, Alam IS, Mayer AT, Gambhir SS, Levy R, Eradication of spontaneous malignancy by local immunotherapy, Sci. Transl. Med 10 (2018), doi:10.1126/scitranslmed.aan4488.

6. Park CG, Hartl CA, Schmid D, Carmona EM, Kim H-J, Goldberg MS, Extended release of perioperative immunotherapy prevents tumor recurrence and eliminates metastases, Sci. Transl. Med 10 (2018), doi:10.1126/scitranslmed.aar1916.

7. Riegler J, Labyed Y, Rosenzweig S, Javinal V, Castiglioni A, Dominguez CX, Long JE, Li Q, Sandoval W, Junttila MR, Turley SJ, Schartner J, Carano RAD, Tumor Elastography and Its Association with Collagen and the Tumor Microenvironment, Clin. Cancer Res (2018), doi:10.1158/1078-0432.CCR-17-3262.

8. Naba A, Clauser KR, Ding H, Whittaker CA, Carr SA, Hynes RO, The extracellular matrix: Tools and insights for the "omics" era, Matrix Biol. 49, 10–24 (2016). [PubMed: 26163349]

9. Nishi N, Matsushita O, Yuube K, Miyanaka H, Okabe A, Wada F, Collagen-binding growth factors: Production and characterization of functional fusion proteins having a collagen-binding domain, Proceedings of the National Academy of Sciences 95, 7018–7023 (1998).

10. Sekiguchi H, Uchida K, Matsushita O, Inoue G, Nishi N, Masuda R, Hamamoto N, Koide T, Shoji S, Takaso M, Basic Fibroblast Growth Factor Fused with Tandem Collagen-Binding Domains from Collagenase ColG Increases Bone Formation, Biomed Res. Int 2018, 8393194 (2018). [PubMed: 29770338]

11. Martino MM, Tortelli F, Mochizuki M, Traub S, Ben-David D, Kuhn GA, Müller R, Livne E, Eming SA, Hubbell JA, Engineering the growth factor microenvironment with fibronectin domains to promote wound and bone tissue healing, Sci. Transl. Med 3, 100ra89 (2011).

12. Nikitovic D, Katonis P, Tsatsakis A, Karamanos NK, Tzanakakis GN, Lumican, a small leucine-rich proteoglycan, IUBMB Life 60, 818–823 (2008). [PubMed: 18949819]

13. Aper SJA, van Spreeuwel ACC, van Turnhout MC, van der Linden AJ, Pieters PA, van der Zon NLL, de la Rambelje SL, Bouten CVC, Merkx M, Colorful protein-based fluorescent probes for collagen imaging, PLoS One 9, e114983 (2014). [PubMed: 25490719]

14. Scott PG, Dodd CM, Bergmann EM, Sheehan JK, Bishop PN, Crystal Structure of the Biglycan Dimer and Evidence That Dimerization Is Essential for Folding and Stability of Class I Small Leucine-rich Repeat Proteoglycans, Journal of Biological Chemistry 281, 13324–13332 (2006).

15. Boyman O, Sprent J, The role of interleukin-2 during homeostasis and activation of the immune system, Nat. Rev. Immunol 12, 180–190 (2012). [PubMed: 22343569]

16. Zhu EF, Gai SA, Opel CF, Kwan BH, Surana R, Mihm MC, Kauke MJ, Moynihan KD, Angelini A, Williams RT, Stephan MT, Kim JS, Yaffe MB, Irvine DJ, Weiner LM, Dranoff G, Wittrup KD, Synergistic innate and adaptive immune response to combination immunotherapy with anti-tumor antigen antibodies and extended serum half-life IL-2, Cancer Cell 27, 489–501 (2015). [PubMed: 25873172]

17. Kwan BH, Zhu EF, Tzeng A, Sugito HR, Eltahir AA, Ma B, Delaney MK, Murphy PA, Kauke MJ, Angelini A, Momin N, Mehta NK, Maragh AM, Hynes RO, Dranoff G, Cochran JR, Wittrup KD, Integrin-targeted cancer immunotherapy elicits protective adaptive immune responses, J. Exp. Med 214, 1679–1690 (2017). [PubMed: 28473400]

18. Moynihan KD, Opel CF, Szeto GL, Tzeng A, Zhu EF, Engreitz JM, Williams RT, Rakhra K, Zhang MH, Rothschilds AM, Kumari S, Kelly RL, Kwan BH, Abraham W, Hu K, Mehta NK, Kauke MJ, Suh H, Cochran JR, Lauffenburger DA, Wittrup KD, Irvine DJ, Eradication of large established tumors in mice by combination immunotherapy that engages innate and adaptive immune responses, Nat. Med 22, 1402–1410 (2016). [PubMed: 27775706]

19. Kontermann RE, Strategies for extended serum half-life of protein therapeutics, Curr. Opin. Biotechnol 22, 868–876 (2011). [PubMed: 21862310]

20. Tzeng A, Kwan BH, Opel CF, Navaratna T, Wittrup KD, Antigen specificity can be irrelevant to immunocytokine efficacy and biodistribution, Proc. Natl. Acad. Sci. U. S. A 112, 3320–3325 (2015). [PubMed: 25733854]

21. Gogas H, Ioannovich J, Dafni U, Stavropoulou-Giokas C, Frangia K, Tsoutsos D, Panagiotou P, Polyzos A, Papadopoulos O, Stratigos A, Markopoulos C, Bafaloukos D, Pectasides D, Fountzilas G, Kirkwood JM, Prognostic significance of autoimmunity during treatment of melanoma with interferon, N. Engl. J. Med 354, 709–718 (2006). [PubMed: 16481638]

22. Spitzer MH, Carmi Y, Reticker-Flynn NE, Kwek SS, Madhireddy D, Martins MM, Gherardini PF, Prestwood TR, Chabon J, Bendall SC, Fong L, Nolan GP, Engleman EG, Systemic Immunity Is Required for Effective Cancer Immunotherapy, Cell 168, 487–502.e15 (2017). [PubMed: 28111070]

23. Poleszczuk JT, Luddy KA, Prokopiou S, Robertson-Tessi M, Moros EG, Fishman M, Djeu JY, Finkelstein SE, Enderling H, Abscopal Benefits of Localized Radiotherapy Depend on Activated T-cell Trafficking and Distribution between Metastatic Lesions, Cancer Res. 76, 1009–1018 (2016). [PubMed: 26833128]

24. Cohen J, IL-12 deaths: explanation and a puzzle, Science 270, 908–908 (1995). [PubMed: 7481785]

25. Leonard JP, Sherman ML, Fisher GL, Buchanan LJ, Larsen G, Atkins MB, Sosman JA, Dutcher JP, Vogelzang NJ, Ryan JL, Effects of single-dose interleukin-12 exposure on interleukin-12-associated toxicity and interferon-gamma production, Blood 90, 2541–2548 (1997). [PubMed: 9326219]

26. Weiss JM, Subleski JJ, Wigginton JM, Wiltrout RH, Immunotherapy of cancer by IL-12-based cytokine combinations, Expert Opin. Biol. Ther 7, 1705–1721 (2007). [PubMed: 17961093]

27. Canton DA, Shirley S, Wright J, Connolly R, Burkart C, Mukhopadhyay A, Twitty C, Qattan KE, Campbell JS, Le MH, Pierce RH, Gargosky S, Daud A, Algazi A, Melanoma treatment with

intratumoral electroporation of tavokinogene telseplasmid (pIL-12, tavokinogene telseplasmid), Immunotherapy 9, 1309–1321 (2017). [PubMed: 29064334]

28. Koneru M, O'Cearbhaill R, Pendharkar S, Spriggs DR, Brentjens RJ, A phase I clinical trial of adoptive T cell therapy using IL-12 secreting MUC-16 ecto directed chimeric antigen receptors for recurrent ovarian cancer, J. Transl. Med 13, 102 (2015). [PubMed: 25890361]

29. Vo JL, Yang L, Kurtz SL, Smith SG, Koppolu BP, Ravindranathan S, Zaharoff DA, Neoadjuvant immunotherapy with chitosan and interleukin-12 to control breast cancer metastasis, Oncoimmunology 3, e968001 (2014). [PubMed: 25964864]

30. Irvine D, Wittrup KD, Mehta NK, Rakhra K, Zhu EF, Protein-chaperoned t-cell vaccines, US Patent (2017) (available at https://patentimages.storage.googleapis.com/e2/36/07/db9c168274ed05/US20170252417A1.pdf).

31. Liu J, Blake SJ, Yong MCR, Harjunpää H, Ngiow SF, Takeda K, Young A, O'Donnell JS, Allen S, Smyth MJ, Teng MWL, Improved Efficacy of Neoadjuvant Compared to Adjuvant Immunotherapy to Eradicate Metastatic Disease, Cancer Discov. 6, 1382–1399 (2016). [PubMed: 27663893]

32. Wigginton JM, Wiltrout RH, IL-12/IL-2 combination cytokine therapy for solid tumours: translation from bench to bedside, Expert Opin. Biol. Ther 2, 513–524 (2002). [PubMed: 12079487]

33. Govaerts AS, Guillaume T, André M, Bayat B, Feyens AM, Hawley TS, Fong AZ, Hawley RG, Symann M, Retroviral-mediated transfer of genes encoding interleukin-2 and interleukin-12 into fibroblasts increases host antitumor responsiveness, Cancer Gene Ther. 6, 447–455 (1999). [PubMed: 10505855]

34. Szabo SJ, Dighe AS, Gubler U, Murphy KM, Regulation of the Interleukin (IL)-12R β2 Subunit Expression in Developing T Helper 1 (Th1) and Th2 Cells, J. Exp. Med 185, 817–824 (1997). [PubMed: 9120387]

35. Starbeck-Miller GR, Xue H-H, Harty JT, IL-12 and type I interferon prolong the division of activated CD8 T cells by maintaining high-affinity IL-2 signaling in vivo, J. Exp. Med 211, 105–120 (2013). [PubMed: 24367005]

36. Gollob JA, Veenstra KG, Parker RA, Mier JW, McDermott DF, Clancy D, Tutin L, Koon H, Atkins MB, Phase I Trial of Concurrent Twice-Weekly Recombinant Human Interleukin-12 Plus Low-Dose IL-2 in Patients With Melanoma or Renal Cell Carcinoma, J. Clin. Oncol 21, 2564–2573 (2003). [PubMed: 12829677]

37. Kaufman HL, Swartout BG, Hörig H, Lubensky I, Combination interleukin-2 and interleukin-12 induces severe gastrointestinal toxicity and epithelial cell apoptosis in mice, Cytokine 17, 43–52 (2002). [PubMed: 11886170]

38. Tugues S, Burkhard SH, Ohs I, Vrohlings M, Nussbaum K, Vom Berg J, Kulig P, Becher B, New insights into IL-12-mediated tumor suppression, Cell Death Differ. 22, 237–246 (2015). [PubMed: 25190142]

39. Smyth MJ, Taniguchi M, Street SE, The anti-tumor activity of IL-12: mechanisms of innate immunity that are model and dose dependent, J. Immunol 165, 2665–2670 (2000). [PubMed: 10946296]

40. Lechner MG, Karimi SS, Barry-Holson K, Angell TE, Murphy KA, Church CH, Ohlfest JR, Hu P, Epstein AL, Immunogenicity of murine solid tumor models as a defining feature of in vivo behavior and response to immunotherapy, J. Immunother. 36, 477–489 (2013). [PubMed: 24145359]

41. Mariathasan S, Turley SJ, Nickles D, Castiglioni A, Yuen K, Wang Y, Kadel III EE, Koeppen H, Astarita JL, Cubas R, Jhunjhunwala S, Banchereau R, Yang Y, Guan Y, Chalouni C, Ziai J, enbabao lu Y, Santoro S, Sheinson D, Hung J, Giltnane JM, Pierce AA, Mesh K, Lianoglou S, Riegler J, Carano RAD, Eriksson P, Höglund M, Somarriba L, Halligan DL, van der Heijden MS, Loriot Y, Rosenberg JE, Fong L, Mellman I, Chen DS, Green M, Derleth C, Fine GD, Hegde PS, Bourgon R, Powles T, TGFβ attenuates tumour response to PD-L1 blockade by contributing to exclusion of T cells, Nature 554, 544–548 (2018). [PubMed: 29443960]

42. Spranger S, Bao R, Gajewski TF, Melanoma-intrinsic β-catenin signalling prevents anti-tumour immunity, Nature 523, 231–235 (2015). [PubMed: 25970248]

43. Postow MA, Callahan MK, Barker CA, Yamada Y, Yuan J, Kitano S, Mu Z, Rasalan T, Adamow M, Ritter E, Sedrak C, Jungbluth AA, Chua R, Yang AS, Roman R-A, Rosner S, Benson B, Allison JP, Lesokhin AM, Gnjatic S, Wolchok JD, Immunologic correlates of the abscopal effect in a patient with melanoma, N. Engl. J. Med 366, 925–931 (2012). [PubMed: 22397654]

44. Wittrup KD, Antitumor Antibodies Can Drive Therapeutic T Cell Responses, Trends Cancer Res. 3, 615–620 (2017).

45. Soerensen MM, Ros W, Rodriguez-Ruiz ME, Robbrecht D, Rohrberg KS, Martin-Liberal J, Lassen UN, Melero Bermejo I, Lolkema MP, Tabernero J, Boetsch C, Piper-Lepoutre H, Waldhauer I, Charo J, Evers S, Teichgräber V, Schellens JHM, Safety PK/PD, and anti-tumor activity of RO6874281, an engineered variant of interleukin-2 (IL-2v) targeted to tumor-associated fibroblasts via binding to fibroblast activation protein (FAP), J. Clin. Orthod 36, e15155–e15155 (2018).

46. Albertini MR, Yang RK, Ranheim EA, Hank JA, Zuleger CL, Weber S, Neuman H, Hartig G, Weigel T, Mahvi D, Henry MB, Quale R, McFarland T, Gan J, Carmichael L, Kim K, Loibner H, Gillies SD, Sondel PM, Pilot trial of the hu14.18-IL2 immunocytokine in patients with completely resectable recurrent stage III or stage IV melanoma, Cancer Immunol. Immunother 67, 1647–1658 (2018). [PubMed: 30073390]

47. List T, Neri D, Biodistribution studies with tumor-targeting bispecific antibodies reveal selective accumulation at the tumor site, MAbs 4, 775–783 (2012). [PubMed: 23032949]

48. Scott AM, Allison JP, Wolchok JD, Monoclonal antibodies in cancer therapy, Cancer Immun. 12, 14 (2012). [PubMed: 22896759]

49. Toyama BH, Savas JN, Park SK, Harris MS, Ingolia NT, Yates JR 3rd, Hetzer MW, Identification of long-lived proteins reveals exceptional stability of essential cellular structures, Cell 154, 971–982 (2013). [PubMed: 23993091]

50. Danielli R, Patuzzo R, Di Giacomo AM, Gallino G, Maurichi A, Di Florio A, Cutaia O, Lazzeri A, Fazio C, Miracco C, Giovannoni L, Elia G, Neri D, Maio M, Santinami M, Intralesional administration of L19-IL2/L19-TNF in stage III or stage IVM1a melanoma patients: results of a phase II study, Cancer Immunol. Immunother 64, 999–1009 (2015). [PubMed: 25971540]

51. Weide B, Neri D, Elia G, Intralesional treatment of metastatic melanoma: a review of therapeutic options, Cancer Immunol. Immunother 66, 647–656 (2017). [PubMed: 28078357]

52. Frey K, Fiechter M, Schwager K, Belloni B, Barysch MJ, Neri D, Dummer R, Different patterns of fibronectin and tenascin-C splice variants expression in primary and metastatic melanoma lesions, Exp. Dermatol 20, 685–688 (2011). [PubMed: 21649738]

53. Afik R, Zigmond E, Vugman M, Klepfish M, Shimshoni E, Pasmanik-Chor M, Shenoy A, Bassat E, Halpern Z, Geiger T, Sagi I, Varol C, Tumor macrophages are pivotal constructors of tumor collagenous matrix, J. Exp. Med 213, 2315–2331 (2016). [PubMed: 27697834]

54. Conklin MW, Eickhoff JC, Riching KM, Pehlke CA, Eliceiri KW, Provenzano PP, Friedl A, Keely PJ, Aligned collagen is a prognostic signature for survival in human breast carcinoma, Am. J. Pathol 178, 1221–1232 (2011). [PubMed: 21356373]

55. Blockhuys S, Agarwal NR, Hildesjö C, Jarlsfelt I, Wittung-Stafshede P, Sun X-F, Second harmonic generation for collagen I characterization in rectal cancer patients with and without preoperative radiotherapy, J. Biomed. Opt 22, 1–6 (2017).

56. Rohani P, Yaroslavsky AN, Feng X, Jermain P, Shaath T, Neel VA, Collagen disruption as a marker for basal cell carcinoma in presurgical margin detection, Lasers Surg. Med (2018), doi:10.1002/lsm.22948.

57. Bindea G, Mlecnik B, Tosolini M, Kirilovsky A, Waldner M, Obenauf AC, Angell H, Fredriksen T, Lafontaine L, Berger A, Bruneval P, Fridman WH, Becker C, Pagès F, Speicher MR, Trajanoski Z, Galon J, Spatiotemporal Dynamics of Intratumoral Immune Cells Reveal the Immune Landscape in Human Cancer, Immunity 39, 782–795 (2013). [PubMed: 24138885]

58. Wolf K, Müller R, Borgmann S, Bröcker E-B, Friedl P, Amoeboid shape change and contact guidance: T-lymphocyte crawling through fibrillar collagen is independent of matrix remodeling by MMPs and other proteases, Blood 102, 3262–3269 (2003). [PubMed: 12855577]

59. Miller JD, Clabaugh SE, Smith DR, Stevens RB, Wrenshall LE, Interleukin-2 is present in human blood vessels and released in biologically active form by heparanase, Immunol. Cell Biol 90, 159–167 (2012). [PubMed: 21606942]

60. Corti A, Curnis F, Rossoni G, Marcucci F, Gregorc V, Peptide-Mediated Targeting of Cytokines to Tumor Vasculature: The NGR-hTNF Example, BioDrugs 27, 591–603 (2013). [PubMed: 23743670]

61. Corrales L, Glickman LH, McWhirter SM, Kanne DB, Sivick KE, Katibah GE, Woo S-R, Lemmens E, Banda T, Leong JJ, Metchette K, Dubensky TW Jr, Gajewski TF, Direct Activation of STING in the Tumor Microenvironment Leads to Potent and Systemic Tumor Regression and Immunity, Cell Rep. 11, 1018–1030 (2015). [PubMed: 25959818]

62. Andtbacka RHI, Kaufman HL, Collichio F, Amatruda T, Senzer N, Chesney J, Delman KA, Spitler LE, Puzanov I, Agarwala SS, Milhem M, Cranmer L, Curti B, Lewis K, Ross M, Guthrie T, Linette GP, Daniels GA, Harrington K, Middleton MR, Miller WH Jr, Zager JS, Ye Y, Yao B, Li A, Doleman S, VanderWalde A, Gansert J, Coffin RS, Talimogene Laherparepvec Improves Durable Response Rate in Patients With Advanced Melanoma, J. Clin. Oncol 33, 2780–2788 (2015). [PubMed: 26014293]
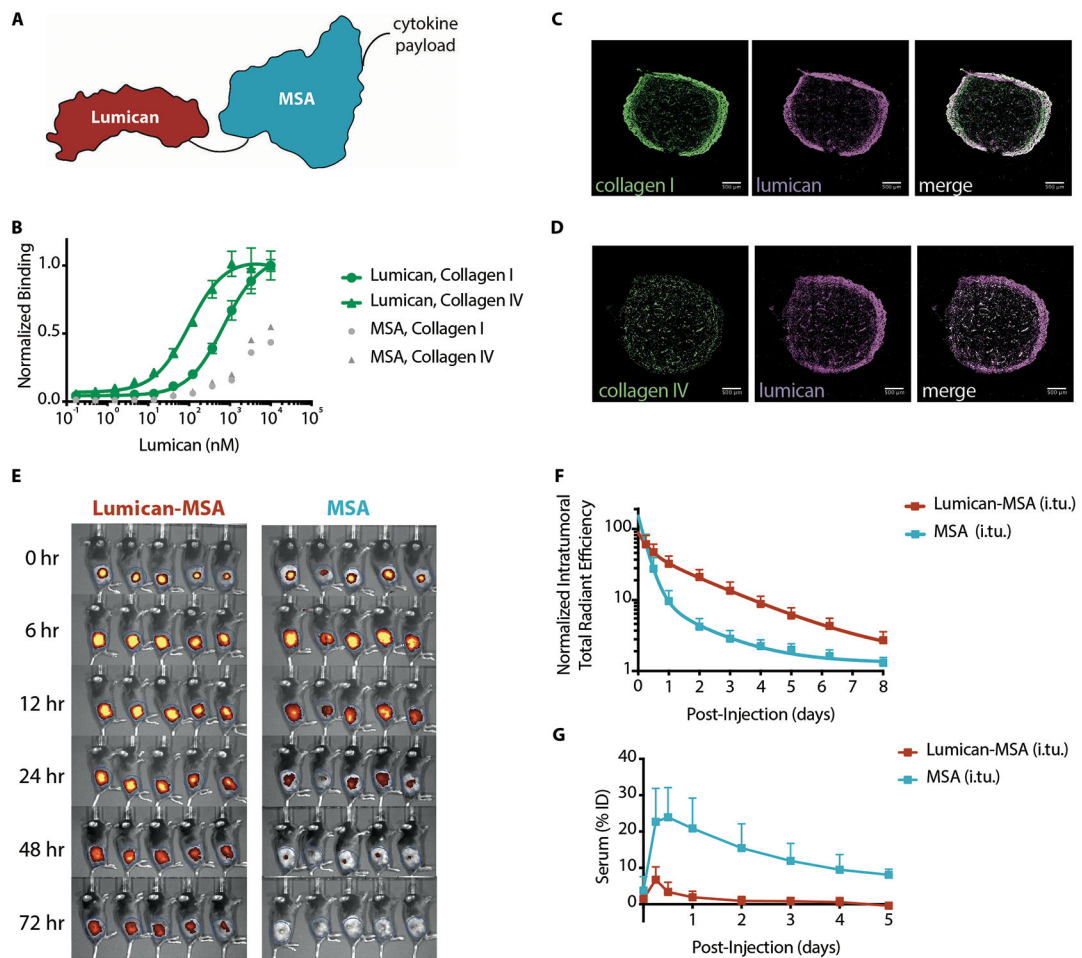
Fig. 1. Lumican binds collagen and demonstrates prolonged retention and systemic isolation after intratumoral injection.
(A) Schematic of a sample fusion protein used to anchor cytokines to intratumoral collagen when locally injected. Black lines represent glycine-serine linkers between collagen-binding protein lumican (red), mouse serum albumin (MSA, blue), and the cytokine. **(B)** Lumican binding to collagen types I and IV was measured by enzyme-linked immunosorbent assay (ELISA) (n = 4, mean +/− S.D.). MSA serves as a nonspecific protein control. **(C and D)** Representative immunofluorescence images of B16F10 tumors excised, fixed, and frozen four days after intratumoral injection of fluorescently labeled Lumican (middle, purple). Sections were stained for either collagen **(C)** type I (left, green) or **(D)** type IV (left, green). White pixels in the merged composites (right) represent areas of colocalization between lumican and the respective collagen stain. Scale bars are 500 μm. **(E)** Images and **(F)** quantification of intratumoral retention and **(G)** serum fluorescence as a percentage of the injected dose (ID) of labeled Lumican-MSA and MSA after injection into B16F10-TRP2KO tumors (n = 5, mean + S.D.).
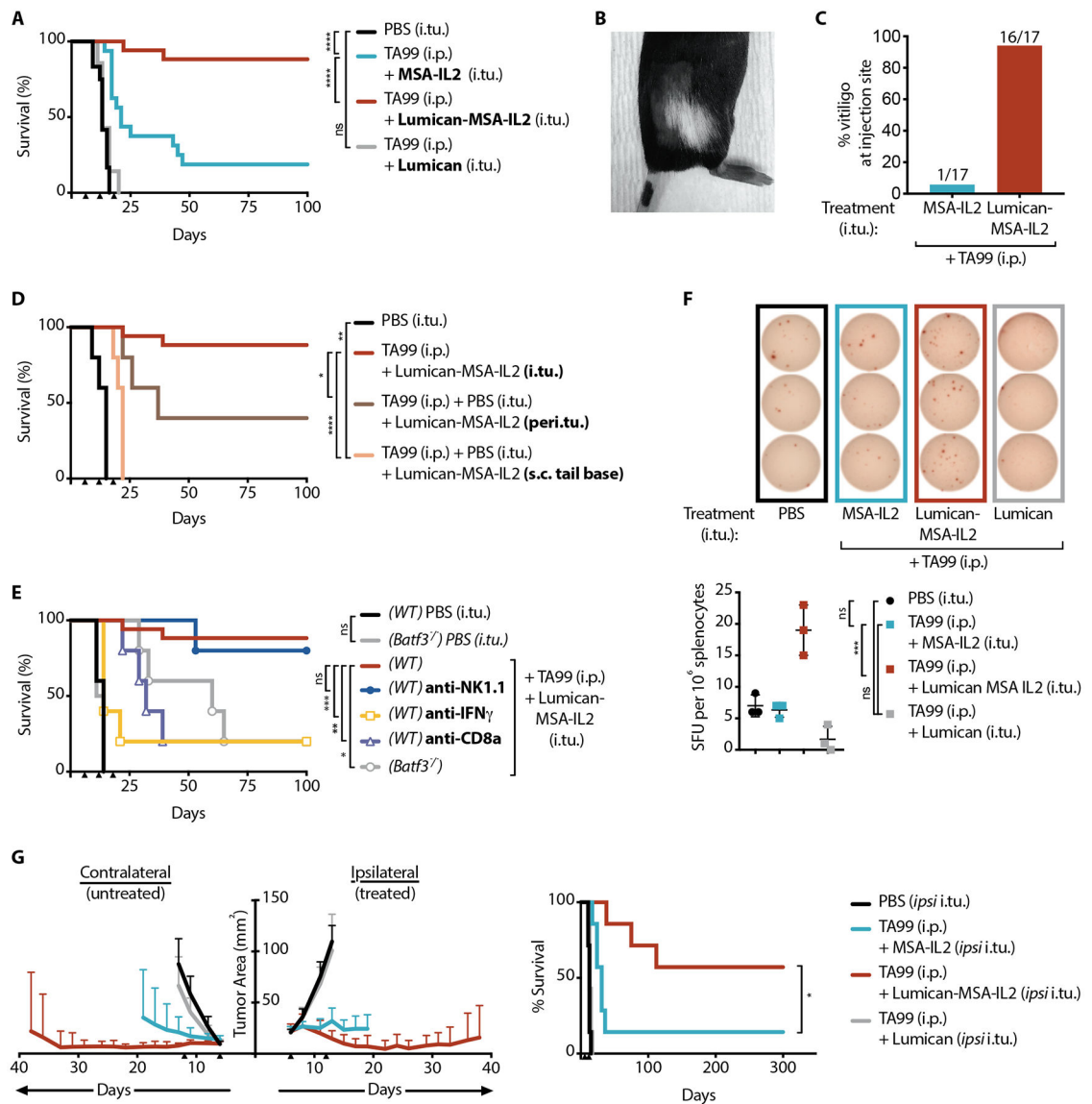
Fig. 2. Anchoring IL-2 to collagen potentiates tumor-targeting antibody TA99.
Mice were inoculated with 1×10^6 B16F10 cells on day 0. **(A)** Survival of these mice treated with intratumoral (i.tu.) injections of PBS (n = 7), MSA-IL2 (n = 17), Lumican (n = 7), or Lumican-MSA-IL2 (n = 17) and intraperitoneal (i.p.) TA99 on days 6, 12, and 18. **(B)** Representative image and **(C)** percentage of treated mice with localized vitiligo after indicated treatment. **(D)** Survival of B16F10 tumor-bearing mice treated with i.p. TA99 and Lumican-MSA-IL2 injected intratumorally (i.tu.) (n = 17), peritumorally (peri.tu.) (n = 5), or 2 cm distal to the lesion subcutaneously at the tail base (s.c. tail base) (n = 5). **(E)** Survival of B16F10 tumor-bearing *Batf3*$^{-/-}$ or wild-type (WT) mice treated with TA99 (i.p.) and Lumican-MSA-IL2 (i.tu.) and with indicated depletion antibody (n = 5/group). **(F)** Representative images (top) of an IFN-γ ELISPOT assay and quantification (bottom) of B16F10-reactive spot-forming units (SFU) from splenocytes isolated four days after the indicated treatments (n = 3/group, mean +/− S.D.). ELISPOT data analyzed by one-way

ANOVA with Tukey's multiple comparison test. **(G)** Study of mice inoculated with 1×10^6 B16F10 cells on the right flank (ipsilateral) and with 3×10^5 B16F10 cells on the left flank (contralateral) on day 0. Ipsilateral intratumoral treatments were administered alongside i.p. TA99 on days 6 and 12. Tumor area (left, mean + S.D.) of the contralateral (untreated) and ipsilateral (treated) lesions and survival (right) were monitored (n = 7/group). Tumor area for each group is shown until a mouse in the group reaches the euthanasia criterion. Arrowheads indicate times of treatment. Survival was compared by log-rank Mantel-Cox test. *, $P < 0.03$; **, $P < 0.002$; ***, $P < 0.0002$; ****, $P < 0.0001$; n.s., not significant.
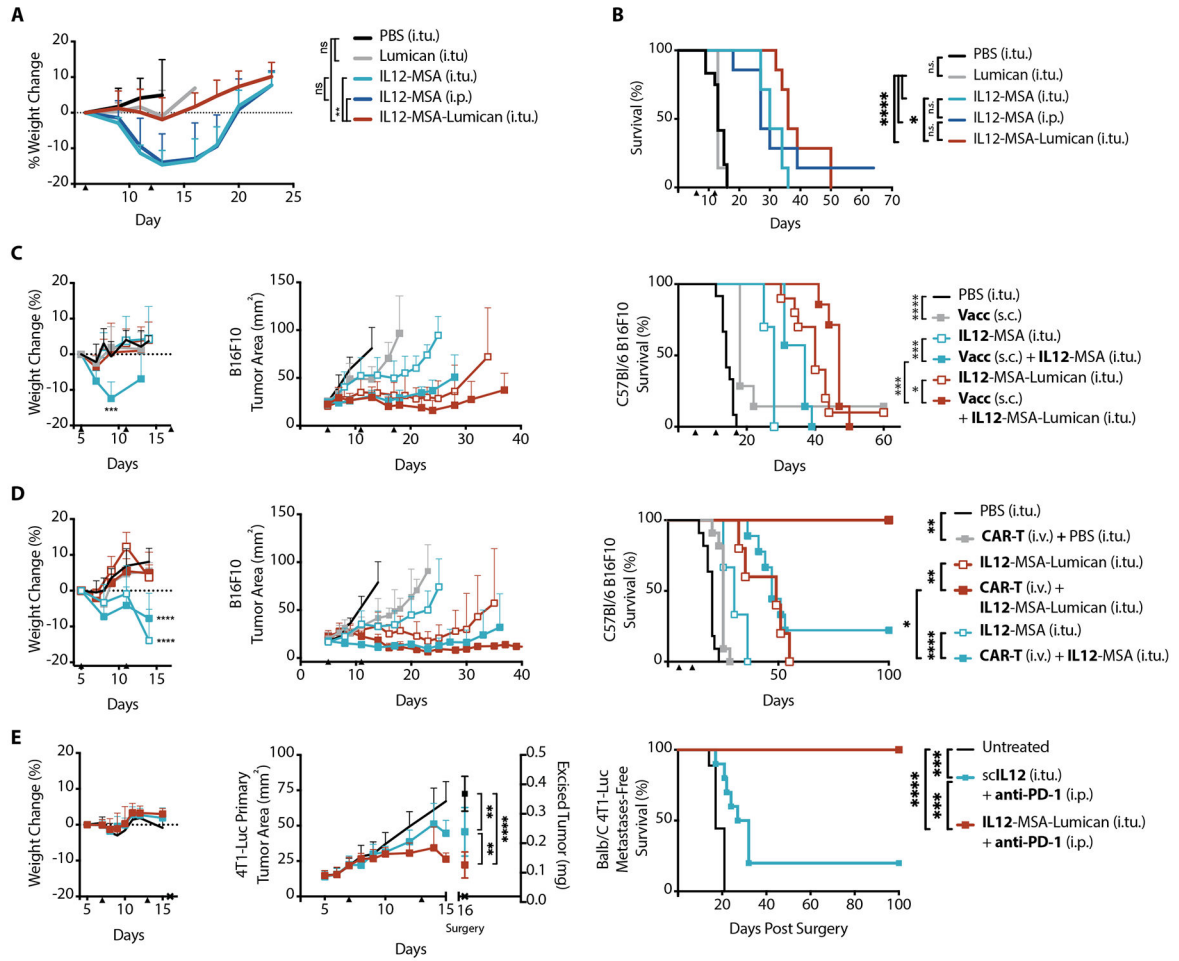
Fig. 3. Collagen-anchoring IL-12 demonstrates reduced toxicity and potentiates disparate systemic immunotherapy modalities.

Mice were inoculated with 1×10^6 B16F10 cells on day 0. **(A)** Weight change from baseline and **(B)** corresponding survival of these mice after treatment with intratumoral (i.tu.) injections of PBS (n = 6), IL12-MSA (n = 7), or IL12-MSA-Lumican (n = 7), or intraperitoneal (i.p.) injection of IL12-MSA (n = 7) on days 6 and 12. Weight change for entire group plotted until a mouse in that group reaches the euthanasia criterion. **(C)** Mice were inoculated with 1×10^6 B16F10 cells on day 0. Vaccinations (Vacc) were administered subcutaneously (s.c.) at the tail base. The graphs show weight change from baseline (left, mean + S.D.), corresponding tumor area (middle, mean + S.D.), and survival (right) of mice treated with i.tu. injections of PBS (n = 12), IL-12 (n = 10 for IL12-MSA; n = 10 for IL12-MSA-Lumican), vaccine (n = 7) alone, or vaccine and IL12 (n = 7 for IL12-MSA; n = 7 for IL12-MSA-Lumican) on days 5, 11, and 17. **(D)** Mice were inoculated with 0.5×10^6 B16F10 cells on day 0 and lymphodepleted by total body irradiation on day 4. CAR-T treatments using 10 million $CD3^+$ CAR-T cells were injected through the tail vein (i.v.) only on day 5. The graphs show weight change from baseline (left, mean + S.D.), corresponding tumor area (middle, mean + S.D.), and survival (right) of mice treated with intratumoral (i.tu.) injections of PBS (n = 11), IL-12 (n = 9 for IL12-MSA; n = 5 for IL12-MSA-Lumican), CAR-T (n = 11) alone, or CAR-T and IL12 (n = 9 for IL12-MSA; n = 5 for IL12-

MSA-Lumican) on days 5 and 11. **(E)** Mice were inoculated with 0.5 x10^6 4T1-Luc cells in the mammary fat pad on day 0. Neoadjuvant therapy was administered on days 7 and 13 and the primary tumors was surgically excised on day 16. Post-operation, mice were monitored for metastases by in vivo imaging. The graphs show total body weight change during neoadjuvant treatment (left), primary tumor growth and weight (middle), and metastasis-free survival (right) of mice left untreated (n = 10) or treated with intratumoral (i.tu.) injections of IL-12 (n = 10 for scIL12; n = 9 for IL12-MSA-Lumican) and intraperitoneal (i.p.) injection of anti-PD-1 on day 7 and 13. Arrowheads indicate times of treatment. Tumor area for each group shown until a mouse in that group reaches the euthanasia criterion or primary tumor is excised. Weight change shown until a mouse in study reaches the euthanasia criterion or primary tumor is excised. Weight changes and excised tumor weights were compared by one-way ANOVA with Tukey's multiple comparison test. Survival was compared by log-rank Mantel-Cox test. *, $P < 0.03$; **, $P < 0.002$; ***, $P < 0.0002$; ****, $P < 0.0001$; n.s., not significant.

Fig. 4. Collagen-anchored IL-12 and IL-2 safely potentiate anti-PD-1.

Mice were inoculated with 1×10^6 B16F10 cells on day 0. **(A)** Weight change from baseline (left, mean + S.D.) and corresponding survival (right) of B16F10 tumor-bearing mice treated with intratumoral (i.tu.) injections of PBS (n = 5), MSA-IL2 and IL12-MSA (n = 5), or Lumican-MSA-IL2 and IL12-MSA-Lumican (n = 5) on days 5 and 11. Weight change shown until a mouse in study reaches the euthanasia criterion. **(B)** Quantification (top, mean + S.D.) of tumor-infiltrating CD8$^+$ T cells (gated on single cell/live/CD45$^+$/CD3$^+$) on day 11 and their corresponding median fluorescence intensity (MFI) of surface PD-1 (bottom, mean + S.D.) after the indicated treatments on day 5. **(C)** Weight change from baseline (left) and corresponding survival (right) of B16F10 tumor-bearing mice treated with intratumoral (i.tu.) injections of PBS (n = 5), MSA-IL2 and IL12-MSA (n = 5), or Lumican-MSA-IL2 and IL12-MSA-Lumican (n = 5) alongside intraperitoneal (i.p.) anti-PD-1 on days 5 and 11. **(D)** Percentage of treated mice with localized vitiligo after the indicated treatments. Treatment groups for which vitiligo was not observed are not included in this plot. **(E)** Percentage of long-term survivors, treated as indicated, which rejected a re-challenge on day 100 with 10^5 B16F10 cells inoculated on the contralateral flank. **(F and G)** Tumor area (left, mean + S.D.) and survival (right) of mice inoculated with **(F)** 1×10^6 EMT6 cells (n = 7 to 14 per group) or **(G)** 1×10^6 MC38 cells (n = 6 to 8 per group) on day 0 and treated as indicated on days 5, 11, and 17. Arrowheads indicate times of treatment. Weights and T cell data were compared by one-way ANOVA with Tukey's multiple comparison test. Survival was compared by log-rank Mantel-Cox test. *, P < 0.03; **, P < 0.002; ***, P < 0.0002; ****, P < 0.0001; n.s., not significant.
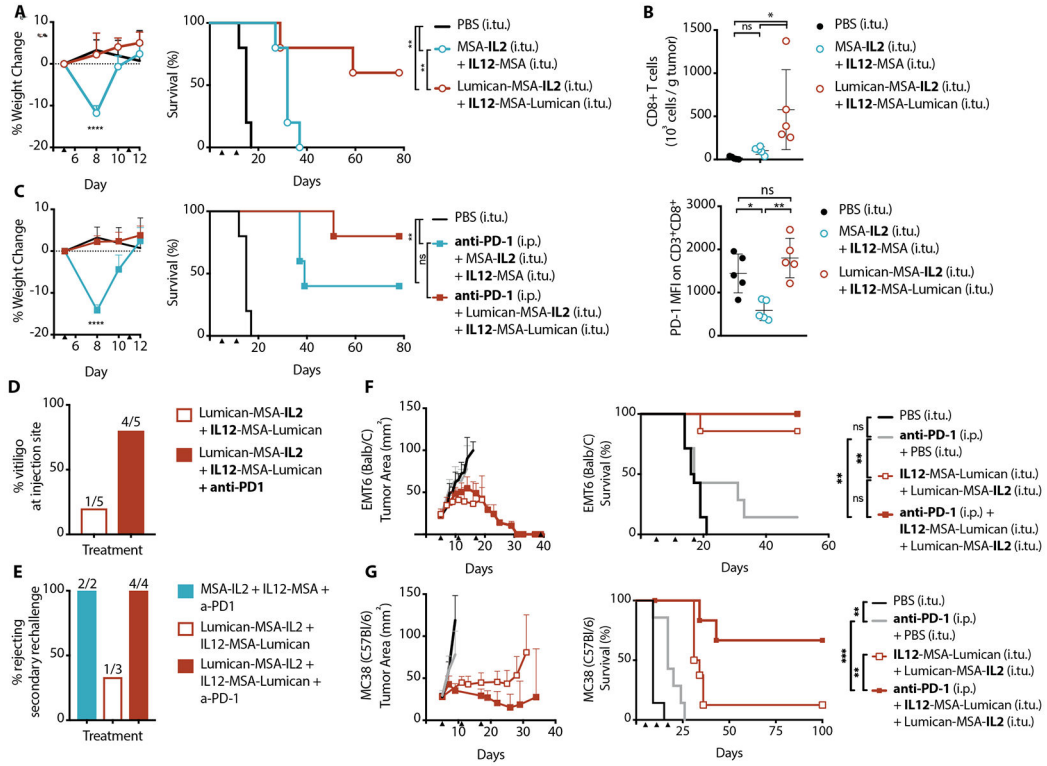
Fig. 5. Collagen-anchoring IL-2 and IL-12, anti-PD-1, and TA99 control large $Braf^{V600E}/Pten^{fl/fl}$ tumors.

Melanoma in $Braf^{V600E}/Pten^{fl/fl}$ mice was initiated by application of 4-hydroxytamoxifen on the right flank on day 0. **(A)** Tumor volume (mean + S.D.) of tumor-bearing mice treated either with an intratumoral (i.tu.) injection of PBS (n = 4) or with i.tu. collagen-anchoring cytokines Lumican-MSA-IL2 and IL12-MSA-Lumican and intraperitoneal (i.p.) TA99 and anti-PD-1 (n = 5) on days 25, 31, 37, 43, 49, 55, 61. For each group, tumor volume shown until a mouse reaches the euthanasia criterion (>1200 mm^3). **(B)** Representative images of $Braf^{V600E}/Pten^{fl/fl}$ flank tumors at onset of indicated treatment on day 25 (top) and before the sixth treatment on day 55 (bottom). **(C)** Overall survival of tumor-bearing mice treated with i.tu. PBS (n = 10), with i.tu. Lumican-MSA-IL2 and IL12-MSA-Lumican and i.p. TA99 and anti-PD-1 (n = 14), with i.tu. Lumican-MSA-IL2 and IL12-MSA-Lumican and i.p. anti-PD-1 (n = 10), with i.tu. MSA-IL2 and IL12-MSA and i.p. TA99 and anti-PD-1 (n = 9), or with i.tu. MSA-IL2 and IL12-MSA and i.p. anti-PD-1 (n = 8) on day 25, 31, 37, 43, 49, 55, 61. Arrowheads indicate times of treatment. Overall survival graph enumerates mice that succumbed to tumor burden (>1200 mm^3) or to treatment-related weight loss (>20%); the latter is indicated by a blue X for each mouse. Survival was compared by log-rank Mantel-Cox test. *, P < 0.03; ***, P < 0.0002; ****, P < 0.0001; n.s., not significant.